Available online at www.sciencedirect.com
SCIENCE DIRECT®
Journal of Nuclear Materials 337–339 (2005) 712–716
journal of nuclear materials
www.elsevier.com/locate/jnucmat

Parallel and radial transport of ELM plasma in the SOL and divertor of JT-60U

N. Asakura *, M. Takechi, N. Oyama, T. Nakano

Naka Fusion Research Establishment, Japan Atomic Energy Research Institute, Naka-machi, Naka-gun, Ibaraki-ken 311-0193, Japan

Abstract

Parallel and radial transport of ELMs in the Scrape-Off-Layer and divertor were investigated in JT-60U. The time lag from the start of magnetic fluctuations to the peak of the ion saturation current (j_s) at low-field-side (LFS) divertor was consistent with convective transport of the ELM plasma along field lines. However, the time lag to the start of the j_s enhancement was shorter than the convection time between the LFS midplane and divertor. In addition, j_s started to increase both at high-field-side and LFS divertors simultaneously, which is not explained by the convection model. Large multi-peaks appeared in the time traces of j_s at the midplane and near the X-point. The radial distribution of the first peak show that the ELM particle flux is transported to outer SOL flux surfaces up to 15 cm from the separatrix. The radial expansion speed at the midplane was in the range of 1–2.5 km/s.

PACS: 52.25.−b
Keywords: Particle heat transport; ELM; Divertor plasma; SOL plasma; JT-60U; Reciprocating probe

1. Introduction

Transient heat and particle loading on the plasma facing components caused by edge localized mode (ELM) events is crucial for determining the lifetime of ITER divertor materials. Recent progress in understanding ELM heat and particle transport from the edge to the divertor has allowed the determination of ELM energy losses and dynamics [1]. It was found that both convection and conduction play an important role in determining transient heat fluxes in the scrape-off-layer (SOL) [2]. A radial transport model of the ELM plasma has been applied to the problem of determining the heat and particle loading to the first wall [3]. The radial and parallel transport of the ELM plasma has been investigated in JT-60U, using Langmuir probes and magnetic pick-up coils. The data acquisition systems for the divertor probes and magnetic pick-up coils were recently improved to achieve a fast sampling rate (200 kHz), which is the same as that for the reciprocating Mach probes at low-field-side (LFS) midplane and X-point and also for the D_α photomultiplier tube (PMT) array [2].

The main parameters for the ELMy H-mode plasmas described in this paper were $I_p = 1$ MA, $B_t = 2$ T, $P_{NB} = 4.3$ MW, and line-averaged electron density of 1.7×10^{19} m^{-3}. The type-I ELM frequency was in the range of 25–40 Hz. 20–30 ELM events were measured over the path of the LFS reciprocating probe scan (25 cm reciprocation during 1 second).

* Corresponding author. Tel.: +81 29 270 7613; fax: +81 029 270 7419/7339.
E-mail address: asakuran@fusion.naka.jaeri.go.jp (N. Asakura).

0022-3115/$ - see front matter © 2004 Published by Elsevier B.V.
doi:10.1016/j.jnucmat.2004.10.164

2. Parallel transport of ELM plasma in SOL and divertor

Rapid changes in the divertor plasma and the parallel transport during ELM heat deposition were investigated. The heat flux to the divertor plate was measured with an infrared TV camera. The time evolution of ion saturation currents at the high-field-side (HFS) and LFS strike points (j_s^{div}), D_α brightness signals, and the peak heat flux densities are shown in Fig. 1. After ELM events, all signals are enhanced. At the HFS strike point, two peaks are observed in j_s^{div} after which there is a fast decay time of 2–3 ms (D_α brightness as well) followed by a slow decrease to their base levels in ~10–15 ms. We investigate rapid changes in the divertor and SOL plasmas during the heat deposition corresponding to one frame of the IRTV (250 μs).

2.1. Plasma propagation in SOL and divertor

Changes in j_s at the LFS midplane, X-point and divertor at an ELM event (t = 5862.5–5864.0 ms) are shown in Fig. 2. Distances from the separatrix for the j_s^{Xp} and j_s^{div} measurements are mapped to the same flux surfaces at the LFS midplane, i.e. Δr^{mid} = 0.3 and 5.3 cm, respectively. The collapse of the electron density pedestal was observed during the early period of large magnetic fluctuations [4]. We assume that the start of rapid and large magnetic fluctuations (t_0^{MHD} = 5862.98 ms) is the start of particle exhaust into SOL. Time lags from t_0^{MHD} to the starts of j_s^{mid} and j_s^{div} enhancements (t_0^{mid} = 5863.03 ms and t_0^{div} = 5863.10 ms) are different. At the same time, large multi-peaks are observed, in particular, for j_s^{mid}. The time lag to the first peak in j_s^{mid} is defined as a radial transport time, τ_{perp}^{mid}. On the other hand, multi-peaks in j_s^{div} are relatively small, and the enhancement of the j_s^{div} above its base level starts 50–100 μs after the first peak in j_s^{mid}. The time lag to the start of the j_s^{div} enhancement is defined as parallel transport time, τ_{para}^{div}. In Fig. 2, τ_{perp}^{mid} and τ_{para}^{div} are 50 and 120 μs, respectively. This shows that the radial transport of the ELM plasma to Δr^{mid} = 5.3 cm is faster than the parallel transport to the LFS divertor. It should be noted that multi-peaks of j_s^{mid} may not extend far along the magnetic field lines since the corresponding multi-peaks were not observed by the D_α PMT array, at a toroidal separation of 90°, as shown in Fig. 2(e).

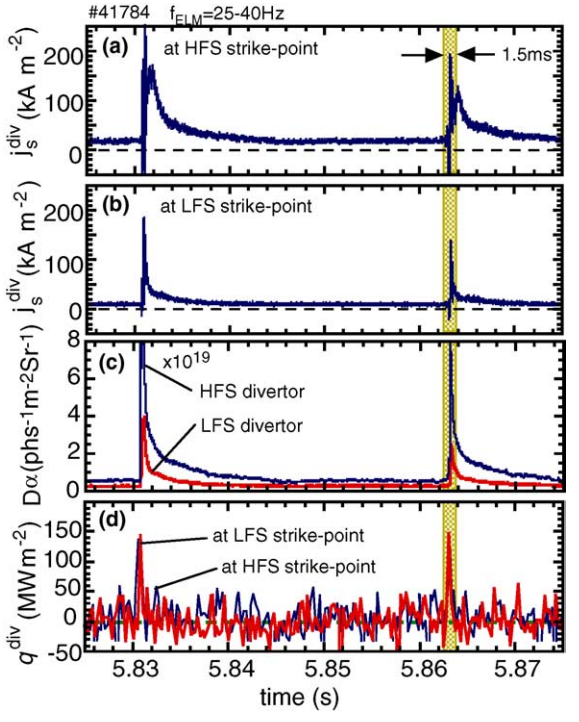

Fig. 1. Data for ELMy H-mode plasmas. Time evolution of ion saturation currents (a) at the high-field-side and (b) low-field-side strike points, (c) D_α brightness at HFS and LFS divertors and (c) peak heat flux densities at HFS and LFS divertors.

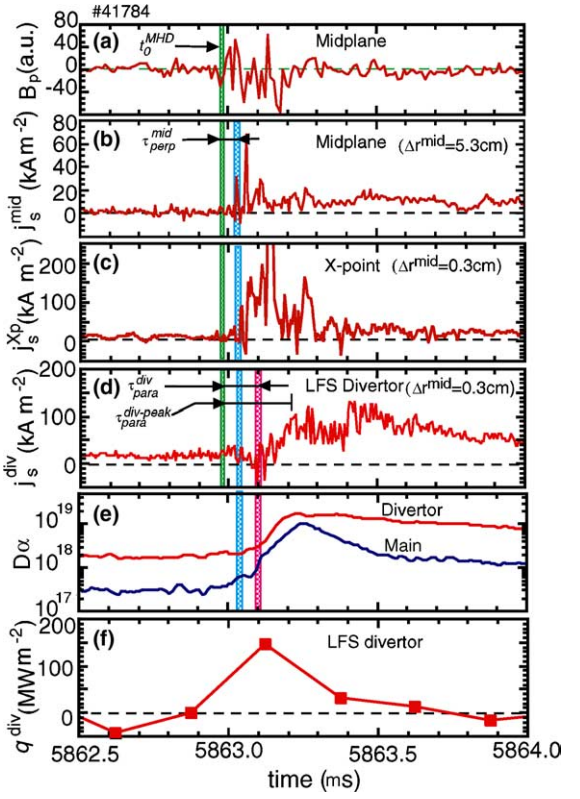

Fig. 2. Enlarged time evolutions of (a) magnetic coil signal at LFS midplane, (b) j_s at LFS midplane, (c) j_s at X-point, (d) j_s at LFS divertor, (e) D_α brightness at main plasma and LFS divertor and (f) heat flux densities at LFS divertor. Start of large magnetic fluctuations, t_0^{MHD}, and time lags from t_0^{MHD} to 1st peak in j_s^{mid}, start of j_s^{div} and j_s^{div} peak are shown by arrows.

The enhancement of the j_s^{mid} base level ($t \sim 5863.1$ ms) appears toroidally symmetric since it occurs at the same time as the rapid rise of the D_α brightness from the main plasma edge.

The statistical distribution of τ_{para}^{div} is shown in Fig. 3. The spread in τ_{para}^{div} is due to the variation of the transient plasma profiles caused by the toroidal and poloidal asymmetries of the ELM structure. About 70% of ELM events are observed in a range of $\tau_{para}^{div} = 70$–130 μs. The time lag to the j_s^{div} peak, $\tau_{para}^{div\text{-}peak}$, is longer than τ_{para}^{div}, corresponding to values in the range 150–190 μs. The plasma convection time along the magnetic field lines is evaluated by $\tau_{para}^{SOL\text{-}LFS}$ $(=L_c^{mid}/C_s) = 140$ μs, where L_c^{mid} (=35 m) is the connection length from the LFS midplane to divertor, and C_s is the plasma sound velocity ($=2.5 \times 10^5$ m/s) for the pedestal plasma ($T_i^{ped} = 800$ eV and $T_e^{ped} = 600$ eV). $\tau_{para}^{div\text{-}peak}$ is slightly longer than $\tau_{para}^{SOL\text{-}LFS}$. Since the electron transit time is a factor of 40 faster than $\tau_{para}^{SOL\text{-}LFS}$, the j_s^{div} peak is consistent with a convective transport model. Note that most τ_{para}^{div} values are shorter than $\tau_{para}^{SOL\text{-}LFS}$, and that the minimum in τ_{para}^{div} is comparable to the convection time from the X-point to the LFS divertor, i.e. $L_c^{Xp}/C_s = 36$ μs, where $L_c^{Xp} = 9$ m. This implies that a part of the ELM enters the SOL below the midplane. The variation of τ_{para}^{div} and $\tau_{para}^{div\text{-}peak}$ may be explained by the variation of the ELM size at the plasma edge. The neutral release from the target due to an increase in the surface temperature by conductive heat load may be another candidate for explaining the early enhancement of j_s^{div}.

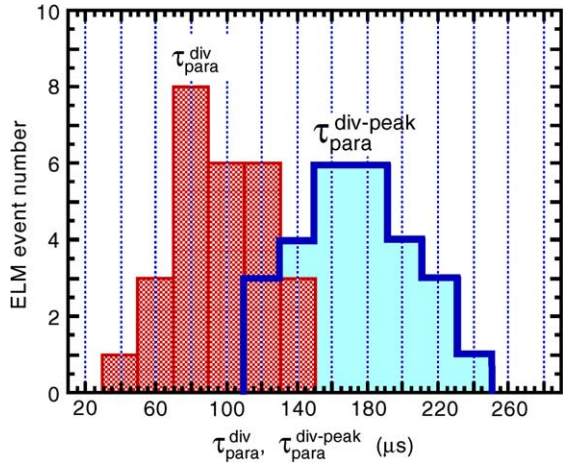

Fig. 3. Distributions of time lags from t_0^{MHD} to start of j_s^{div} (τ_{para}^{div}) and j_s^{div} peak ($\tau_{para}^{div\text{-}peak}$) are shown. Thick bar steps show τ_{para}^{div} and $\tau_{para}^{div\text{-}peak}$ respectively.

2.2. ELM plasma at HFS and LFS divertors

The time evolutions of j_s^{div} near the HFS and LFS strike-points and D_α brightness signals are shown in Fig. 4. Perhaps surprisingly, it is found that j_s^{div} at the HFS and LFS strike-points are enhanced simultaneously, and that large *negative* j_s^{div} (i.e. implying net electron current) is observed in the private flux region, in particular, near the HFS strike-point: the peak j_s^{div} is -150 k Am^{-2} at HFS and -70 k Am^{-2} at LFS when the probes are biased to -180 V. When the probes were electrically floated from the divertor target (in similar shots), a large negative floating potential (V_f) of up to -500 V was observed at the HFS private region. This implies that fast electrons larger than the probe bias are deposited on the probe during an ELM.

Assuming a convection transport model the plasma convection time from the LFS midplane to the HFS divertor, $\tau_{para}^{SOL\text{-}HFS}$, is expected to be 330 μs, which is 2.4 times longer than $\tau_{para}^{SOL\text{-}LFS}$. Thus the fast j_s^{div} enhancement at the HFS strike-point is not explained by the convection model. Neutral release and prompt ionization due to the conduction heat load may be an explanation of the fast HFS j_s^{div} rise. Another explanation could be the large enhancement in the *negative* j_s^{div} at the private flux region which suggests deposition of fast electrons. This would lead to an enhancement of the negative sheath potential due to secondary electron emission [5]. However, the fast electrons arriving

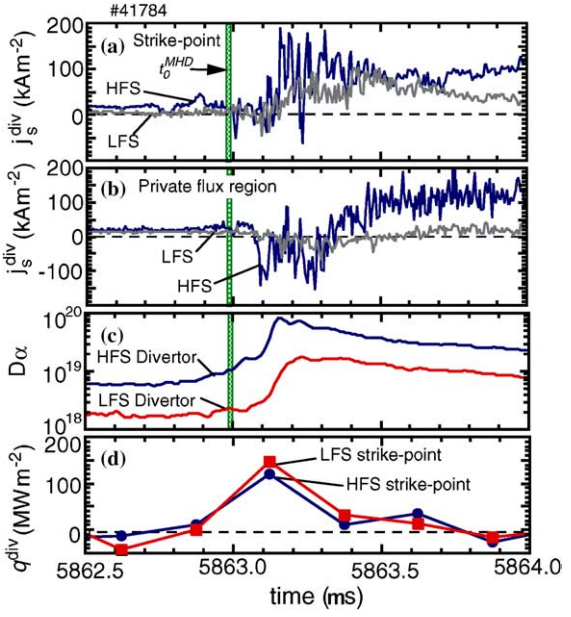

Fig. 4. Enlarged time evolutions of (a) j_s at strike points, (b) j_s at private flux region, (c) D_α brightness, (d) peak heat flux densities, in HFS and LFS divertors. Start of large magnetic fluctuations, t_0^{MHD}, is shown by a vertical line.

in the private region are not yet explained. After $\tau_{para}^{SOL\text{-}HFS}$, j_s^{div} at the HFS private region becomes positive with magnitude comparable to that at the strike-point. Both the convective flux and the E × B drift flow in the private region presumably travel to the HFS divertor.

3. Radial transport of ELM plasma

The radial propagation of ELMs through the SOL has been investigated using probes at the LFS midplane and X-point. Fig. 5 shows time evolutions of j_s^{mid} for Δr^{mid} of 4.4 and 14 cm.

We first describe the radial distribution of the parallel ion flux in the ELM, $\gamma_{i\|}^{mid}$. For each ELM $\gamma_{i\|}^{mid}$ is evaluated from the first few large peaks of j_s^{mid} after t_0^{MHD} : j_s^{mid} peaks at $\Delta t = 42$, 78 μs and at $\Delta t = 79$, 98 μs are used in Fig. 5(a) and (b), respectively. During an ELM event, $\gamma_{i\|}^{mid}$ is enhanced over a wide SOL region as shown in Fig. 6(a). The $\gamma_{i\|}^{mid}$ profile shown is *an envelope of* $\gamma_{i\|}^{mid}$ *peaks* rather than a profile at one moment. Here, the distance between the separatrix and the first wall is 21 cm at the midplane Mach probe. The enhancement of $\gamma_{i\|}^{mid}$ is large near the separatrix (×5–10 for $\Delta r^{mid} < 4$ cm) dropping slightly (× ~ 5) further out in the SOL. The ELM $\gamma_{i\|}^{mid}$ distribution is described by two exponential curves with 1st and 2nd e-folding lengths, λ_γ^{mid}, which are 2.1 and 8.5 cm, respectively.

The peak $\gamma_{i\|}^{Xp}$ values and the $\gamma_{i\|}^{Xp}$ profile between ELMs are shown in Fig. 6(b). Here, the horizontal scan of the X-point Mach probe is 17 cm corresponding to 3.8 cm at the midplane. The enhancement of $\gamma_{i\|}^{Xp}$ is similar to that of $\gamma_{i\|}^{mid}$ near the separatrix (a factor of 5–12).

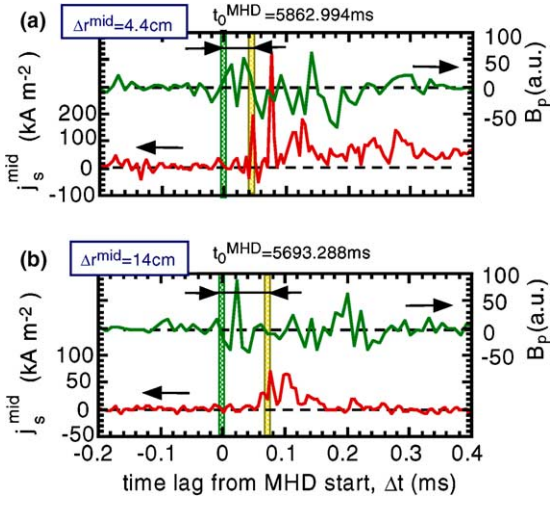

Fig. 5. Enlarged time evolutions of magnetic coil signal and j_s at LFS midplane. Distance from the saparatrix is (a) 4.4 cm and (b) 14 cm. Start of large magnetic fluctuations (t_0^{MHD}) and 1st large peak in j_s are shown by vertical lines.

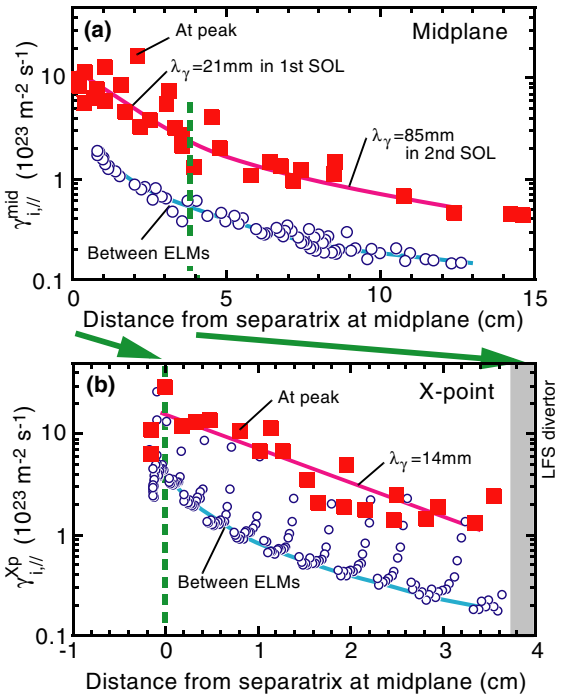

Fig. 6. Distribution of peaks in parallel ion flux ($\gamma_{i,\|}$) during ELM activity, and $\gamma_{i,\|}$ profile between ELMs, (a) at LFS midplane and (b) at X-point. (Upper) Separation from separatrix and first wall at the midplane is 21 cm. (Lower) Separation between separatrix and the divertor is mapped to midplane radius.

The peak $\gamma_{i\|}^{Xp}$ profile is described by one exponential curve with $\lambda_\gamma^{Xp} = 2.1$ cm, also similar to $\gamma_{i\|}^{mid}$.

We next describe the radial velocities of the ELM at the LFS midplane, V_{perp}^{mid}. $V_{perp}^{mid} = \Delta r^{mid}/\tau_{perp}^{mid}$, where τ_{perp}^{mid} is defined as the delay between t_0^{MHD} and the first j_s^{mid} peak. The radial distribution of τ_{perp}^{mid} is shown in Fig. 7. Large multi-peaks in j_s^{mid} are often observed

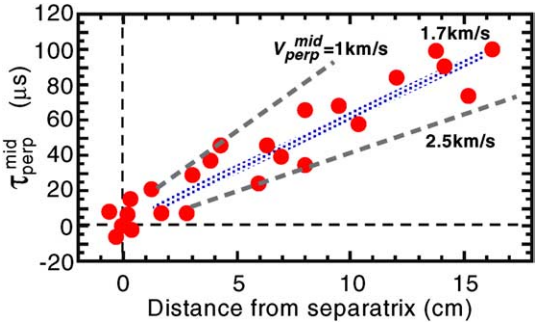

Fig. 7. Distribution of time lags from start of large magnetic fluctuation to 1st large peak in j_s^{mid} (τ_{perp}) are shown. $V_{perp}^{mid} = 1.7$ km/s is determined from linear fit of $\tau_{perp}^{mid} = \Delta r^{mid}/V_{perp}^{mid}$. Lines corresponding to 1 and 2.5 km/s are shown.

for $\Delta r^{\mathrm{mid}} < 8$ cm. If we select only the $\tau_{\mathrm{perp}}^{\mathrm{mid}}$ for the first peak, we see that $\tau_{\mathrm{perp}}^{\mathrm{mid}}$ increases with Δr^{mid}. Since the data has a large scatter near the separatrix, a linear fit of $\tau_{\mathrm{perp}}^{\mathrm{mid}}$ is applied for $\Delta r^{\mathrm{mid}} > 1$ cm. The best fir to this data gives $V_{\mathrm{perp}}^{\mathrm{mid}} = 1.7$ km/s between (range 1–2.5 km/s). This $V_{\mathrm{perp}}^{\mathrm{mid}}$ is larger than those evaluated in JET [3,6]. The peak in $j_{\mathrm{s}}^{\mathrm{mid}}$ corresponding to an ELM has a period of ~ 10 μs. Assuming that the ELM travels outward with a velocity of 1.7 km/s, the radial width of the ELM would be a few cm. A similar radial size of ELM filaments was reported in fast visible and infrared TV cameras [7,8]. The toroidal and poloidal extensions of the ELM plasma, and the plasma temperature must be determined if we are to evaluate the heat flux to the first wall.

4. Summary

The parallel and radial transport of ELMs have been investigated in the SOL and divertor. The time lag to the j_{s} peak at LFS divertor after the ELM start determined from MHD is consistent with parallel convection from LFS midplane to the divertor. It is suggested that the fast start of the $j_{\mathrm{s}}^{\mathrm{div}}$ enhancement is due to the poloidal extent of the ELM and associated plasma exhaust. A convection model is not consistent with two other observations: (1) The rise in $j_{\mathrm{s}}^{\mathrm{div}}$ at HFS strike-point is simultaneous with that of the LFS $j_{\mathrm{s}}^{\mathrm{div}}$ and (2) evidence of fast electrons has been found at the private flux region.

Enhancement and propagation of the peak plasma flux is observed even at outer SOL flux surfaces 16 cm from the separatrix. We have inferred that the ELM has radial velocity of 1.7 km/s (range 1–2.5 km/s), and a radial width of a few cm. Measurements of the toroidal extent of ELMs along the field lines and plasma temperature are needed in the future if the heat load to first wall is to be evaluated from this data.

References

[1] A. Loarte, G. Saibene, R. Sartori, et al., J. Nucl. Mater. 313–316 (2003) 962.
[2] N. Asakura, S. Sakurai, O. Naito, et al., Plasma Phys. Control. Fusion 44 (2002) A313.
[3] W. Fundamanski, W. Sailer, JET EFDA contributors, Plasma Phys. Control. Fusion 46 (2004) 204.
[4] N. Oyama, N. Asakura, A.V. Chankin, et al., Nucl. Fus. 44 (2004) 582.
[5] A. Bergmann, Nucl. Fus. 42 (2002) 1162.
[6] B. Goncalves, C. Hidalgo, M.A. Perosa, et al., Plasma Phys. Control. Fusion 45 (2003) 1627.
[7] A. Kirk et al., 30th EPS Conf. On controlled Fusion and Plasma Physics, St. Petersburg, Russia, 2003, P-3.201.
[8] A. Herrmann, T. Eich, C. Fuchs et al., these Proceedings, doi:10.1016/j.jnucmat.2004.10.126.